



Title	Geometric effects on critical behaviours of the Ising model
Author(s)	Shima, Hiroyuki; Sakaniwa, Yasunori
Citation	Journal of Physics A Mathematical and General, 39(18), 4921-4933 <a href="https://doi.org/10.1088/0305-4470/39/18/010">https://doi.org/10.1088/0305-4470/39/18/010</a>
Issue Date	2006-05-05
Doc URL	<a href="http://hdl.handle.net/2115/14508">http://hdl.handle.net/2115/14508</a>
Type	article (author version)
File Information	JPA_revised.pdf



[Instructions for use](#)

# Geometric effects on critical behaviours of the Ising model

**Hiroyuki Shima and Yasunori Sakaniwa**

Department of Applied Physics, Graduate School of Engineering, Hokkaido University, Sapporo 060-8628, Japan

E-mail: shima@eng.hokudai.ac.jp

**Abstract.** We investigate the critical behaviour of the two-dimensional Ising model defined on a curved surface with a constant negative curvature. Finite-size scaling analysis reveals that the critical exponents for the zero-field magnetic susceptibility and the correlation length deviate from those for the Ising lattice model on a flat plane. Furthermore, when reducing the effects of boundary spins, the values of the critical exponents tend to those derived from the mean field theory. These findings evidence that the underlying geometric character is responsible for the critical properties the Ising model when the lattice is embedded on negatively curved surfaces.

PACS numbers: 05.50.+q, 05.70.Jk, 64.60.Fr, 75.40.Cx

Submitted to: *J. Phys. A: Math. Gen.*

## 1. Introduction

Scaling concept plays a vital role in describing critical phenomena associated with a second-order phase transition. The fundamental hypothesis states that, in the vicinity of a critical point, the largest length scale of the fluctuation of the order parameter diverges and all length scales contribute with equal importance [1, 2]. Theoretical arguments based on this hypothesis explain why most thermodynamic quantities near the critical point exhibit power-law behaviour with characteristic exponents that are independent of the microscopic details of a system [3, 4, 5].

A primary example of a physical model exhibiting a second-order phase transition is the two-dimensional Ising model with ferromagnetic interaction [6, 7, 8]. This model has been used extensively for innumerable projects in statistical physics, mainly due to its simplicity and broad applicability to real systems. Whereas its physical properties have been thoroughly investigated, it still continues to raise interesting issues that are relevant to a wide range of critical phenomena. Most intriguing among them is the critical properties of the Ising model defined on curved geometry [9, 10, 11, 12, 13, 14, 15]. In fact, several studies have been carried out on Ising lattice models with topologies ranging from a torus [6, 9, 16], and sphere [10, 11, 12, 13, 14] to genus two curved surfaces [15], as well as those with Brascamp-Kunz boundary conditions [17, 18]. The results of these studies are consistent with the fact that an alteration in the topology or the boundary condition of the Ising lattice does not change its scaling behaviour, and thus the system remains in the flat-space Onsager universality class [6].

The objective of the current study is to focus on an alternative property of curved geometries — surface *curvature* — instead of their *topology*. Our main concern is whether a uniform change in the constant surface curvature affects the scaling behaviour of the mounted Ising lattice model. It should be noted that in most systems considered thus far, the magnitude of surface curvature is spatially concentrated on a portion of the surface, even producing a conical singularity. This inhomogeneous distribution of local curvature would possibly make it difficult to distinguish the effect of curvature from among other incidental contributions on the critical properties. In addition, when a surface has a closed form (e.g., a sphere), its ability to attain the thermodynamic limit with a constant surface curvature is disabled ‡. This limitation can be removed successfully by employing a surface with a constant negative curvature. This surface, in which the Gaussian curvature possesses a finite constant value at arbitrary points, is simply connected and infinite [19, 20]. Hence, such a surface can serve as an example for considering the geometric effects on the critical properties of the mounted system.

In the present paper, we investigate the critical behaviour of the two-dimensional Ising lattice model defined on a curved surface with a constant negative curvature. Monte Carlo (MC) simulations and finite-size scaling analyses are employed to compute the critical exponent  $\gamma$  for the zero-field magnetic susceptibility and  $\mu$  for the correlation

‡ For example, a sphere reduces to a flat plane at some point within the thermodynamic limit where the effect of curvature is absent.

volume. We demonstrate that the values of both  $\gamma$  and  $\mu$  deviate from those for the planar Ising lattice model, which indicates the relevance of the intrinsic geometry of the underlying surface to the critical properties of the mounted Ising model. Moreover, when reducing the boundary contributions, the values of  $\gamma$  and  $\mu$  exhibit a tendency to shift to those derived from the mean-field approximation. This non-trivial behavior of the critical exponents is qualitatively consistent with the conclusion based on the series expansion analyses [21] and that deduced from the quantum field theory [22]. We also calculate the fourth-order Binder's cumulant that provides a check of the results of finite size scaling.

## 2. Scaling arguments for the Ising model

Let us briefly review the framework of the scaling argument that successfully explains the critical properties of the two-dimensional planar Ising lattice model [3]. The scaling hypothesis states that, in the vicinity of the critical temperature  $T_c$ , the singular part of the free energy  $f_s$  of the Ising lattice per site should be a homogeneous function:

$$\lambda^d f_s(t, h) = f_s(\lambda^x t, \lambda^y h), \quad (1)$$

where  $t = (T - T_c)/T_c$ ,  $h = H/(k_B T)$  and  $H$  represents an external magnetic field. The parameter  $\lambda^d$  with a spatial dimension  $d$  indicates the rescaling of the total number of sites from  $N$  to  $\lambda^d N$ ; this results from the transformation of the linear dimension of the entire Ising lattice:  $L \rightarrow \lambda L$ . By eliminating  $\lambda$  from (1), we obtain the scaling relation of  $f_s$ :

$$f_s(t, h) = |t|^{d/x} \mathcal{F}\left(\frac{h}{|t|^{y/x}}\right), \quad (2)$$

where  $\mathcal{F}$  is a universal scaling function. The appropriate differentiation of (2) yields the power-law form of thermodynamic quantities such as the zero-field susceptibility  $\chi \equiv \partial^2 f_s / \partial h^2 \propto |t|^{-\gamma}$ , where the critical exponents are expressed as functions of  $x$  and  $y$  (for instance,  $\gamma = (2y - d)/x$ ).

Equation (1) is justified when the Ising lattice is defined on a flat plane, since the rescaling of  $L$  by  $\lambda$  is equivalent to that of  $N$  by  $\lambda^d$ . However, this is not the case when the Ising lattice is defined on a curved surface; while a wide range of regular lattices can be constructed on curved surfaces with a constant Gaussian curvature [19, 20], the relation  $N = L^d$  become invalid for these lattices due to the differences in the metric of the underlying geometry. Hence, the rescaling  $L \rightarrow \lambda L$  does not imply  $N \rightarrow \lambda^d N$ , which requires some modifications of (1). §

We thus introduce an alternative rescaling parameter  $\Lambda$  for considering the scaling relation of the Ising model on curved surfaces:

$$\Lambda f_s(t, h) = f_s(\Lambda^{\tilde{x}} t, \Lambda^{\tilde{y}} h), \quad (3)$$

§ Similar argument has been made regarding an infinitely coordinated Ising model; see Ref. [23].

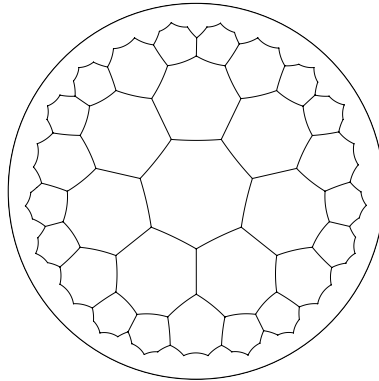


**Figure 1.** Schematic illustration of a regular heptagonal lattice in terms of the Poincaré disk representation. The number of concentric layers of heptagons is  $r = 3$  in this figure. All heptagons depicted within the circle are congruent with respect to the metric given in Eq. (A.3). The circumference corresponds to an infinite distance from the center of the circle.

where  $\Lambda$  represents the rescaling of total sites  $N \rightarrow \Lambda N$ . When the underlying geometry of the lattice is flat, the relation (3) reduces to (1) since  $\Lambda = \lambda^d$ . In this case, the parameters  $\tilde{x}$  and  $\tilde{y}$  given in (3) are defined as  $\tilde{x} = x/d$  and  $\tilde{y} = y/d$ , thus yielding identical values of critical exponents (for instance,  $\tilde{\gamma} = (2\tilde{y} - 1)/\tilde{x} = (2y - d)/x = \gamma$ ). In contrast, when the underlying geometry is curved,  $\Lambda$  can be no longer expressed as a power of  $\lambda$ ; thus,  $\tilde{x}$  and  $\tilde{y}$  are not related to  $x$  and  $y$ . Consequently, the critical exponents for the latter model, which are determined by  $\tilde{x}$  and  $\tilde{y}$ , may quantitatively differ from those for the planar Ising lattice. This naturally motivates us to evaluate the critical exponent directly by constructing the Ising lattice model on curved surfaces.

### 3. Regular tessellation of curved surfaces

A simple spherical surface seems to be the optimal geometry to consider the curvature effect on the critical properties of the Ising model. In fact, a number of efforts have been performed on the Ising model with lattices whose topology is equivalent to a spherical surface [10, 11, 12, 13, 14]. It is noted that, however, the thermodynamic limit cannot be considered for the closed form of sphere-like surfaces having *positive* curvature while maintaining their finite curvature. This is because a spherical surface reduces to a flat plane in this limit, where the curvature effect vanishes completely.

Therefore, instead of a sphere, we consider a curved surface with *negative* constant curvature, termed a *pseudosphere* [19, 20]. The pseudosphere is a simply connected infinite surface in which the Gaussian curvature at arbitrary points possesses a constant negative value. (The definition of the pseudosphere will be given in Appendix.) Hence, it serves as a suitable geometry for considering the curvature effect on the critical properties of a system. It should be noted that the pseudosphere occurs in manifold physical problems ranging from quantum Hall effects [24, 25, 26, 27, 28], quantum chaos

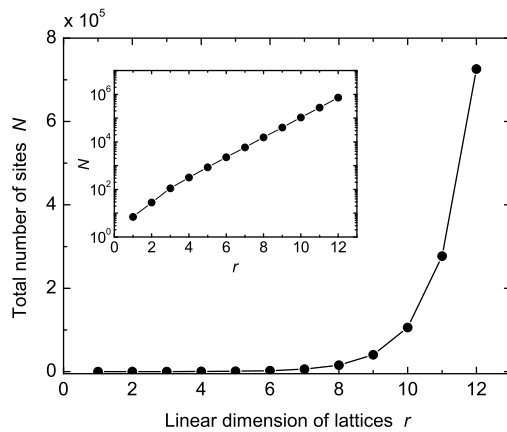


**Figure 2.** Total number of sites  $N$  involved in the heptagonal lattice with various system sizes. The horizontal axis represents the number of concentric layers of heptagons,  $r$ ; this effectively serves as the linear dimension of the entire lattice. Inset: A single logarithm plot of the identical data shown in Fig. 2. It is clearly seen that  $N$  for  $r \gg 1$  increases exponentially with  $r$ .

[29, 30, 31], the string theory [32] to cosmology [33], wherein the underlying geometric character of the system is extremely significant.

Interestingly, a wide range of regular lattices can be constructed on the pseudosphere [20]. This is achieved by a tessellation procedure, where the entire surface is covered by non-overlapping regular polygons meeting only along complete edges or at vertices. It is known that a regular tessellation of the pseudosphere with  $q$  regular  $p$ -sided polygons meeting at each vertex satisfies the following property: [20]

$$(p - 2)(q - 2) > 4. \quad (4)$$

Hence, the series of integer sets  $\{p, q\}$  satisfying (4) results in an infinite number of possible regular tessellations of a pseudosphere. This is in contrast to the case of a flat plane, where only three regular tessellations are allowed:  $\{p, q\} = \{3, 6\}$ ,  $\{4, 4\}$  and  $\{6, 3\}$  satisfying the condition  $(p-2)(q-2) = 4$ . For simplicity, we adopted a heptagonal  $\{7, 3\}$  tessellation to construct the Ising lattice on a pseudosphere. Figure 1 illustrates the local bond structure of a regular heptagonal lattice in terms of the Poincaré disk representation. The resulting lattice comprises concentric layers of congruent heptagons surrounding a central heptagon. The Ising lattice models embedded on a pseudosphere have been considered thus far [21, 34, 35]; however, explicit temperature dependences of thermodynamics quantities close to the transition are yet to be concerned.

Due to a peculiar metric of a pseudosphere, the total number of sites  $N$  of our heptagonal lattice exhibit a non-trivial evolution behaviour with the increase in the lattice size. The size of our lattice is determined by the number of concentric layers of heptagons, denoted by  $r$ , which effectively serves as a linear dimension in our lattice.

For a given  $r$ , the number of total sites  $N$  is expressed as follows:

$$\begin{aligned}
 N(r=1) &= 7, \\
 N(r \geq 2) &= 7 + 7 \sum_{j=0}^{r-2} \left[ c_+ \left( \frac{1+c_+}{2} \right)^j + c_- \left( \frac{1+c_-}{2} \right)^j \right], \quad (5)
 \end{aligned}$$

where  $c_{\pm} = 2 \pm \sqrt{5}$ . Figure 2 plots the dependence of  $N$  on the effective linear dimension  $r$ . When  $r \gg 1$ , it is approximated as  $N(r) \simeq 5 \exp(r)$ ; this means that  $N$  rapidly increases with  $r$  in comparison with the case of the planar Ising model. The exponential increase in  $N(r)$  is a manifestation of the constant negative curvature of the underlying geometry of our lattice.

It should be noted that, when considering thermodynamic properties of our lattice, careful treatments on boundary effects are required. The exponential increase in  $N(r)$  results in that the ratio  $[N(r) - N(r-1)]/N(r)$  approaches a non-zero constant  $1 - e^{-1}$  in the limit  $r \rightarrow \infty$ . This means that the boundaries of our lattices can not be neglected even in the thermodynamic limit, but contain a finite fraction of the total sites. Boundary effects coming from these sites are difficult to be eliminated completely, because the periodic boundary conditions are hard to be employed to regular lattices assigned on a pseudosphere.

In order to extract the bulk critical phenomena, therefore, we have followed the procedure mentioned below. Suppose that an Ising lattice consists of  $r_{\text{out}}$  concentric layers of heptagons. Then, for computing physical quantities of the system (magnetic susceptibilities, for instance), we take into account only the Ising spins involved in the interior  $r_{\text{in}}$  layers ( $r_{\text{in}} \leq r_{\text{out}}$ ) so as to reduce the contribution of the spins locating near the boundary. In actual calculations,  $r_{\text{in}}$  is varied from 4 to 8, and for each  $r_{\text{in}}$  the number of disregarded layers  $\Delta r \equiv r_{\text{out}} - r_{\text{in}}$  is systematically increased from 0 to 4. By investigating the asymptotic behavior of the system for large  $\Delta r$ , we can deduce the bulk properties of the Ising lattice model embedded on the pseudosphere.

#### 4. Numerical methods

We considered the conventional Ising model with ferromagnetic interaction:

$$H = -J \sum_{\langle i,j \rangle} s_i s_j, \quad s_i = \pm 1, \quad (6)$$

where  $\langle i, j \rangle$  denotes a pair of nearest-neighbour sites on a heptagonal lattice. The free boundary condition is imposed for all lattices to be considered. Temperatures and energies are expressed as units of  $J/k_B$  and  $J$ , respectively. The order parameter  $m$  per site for a given configuration of  $\{s_i\}$  is given by  $m = \sum_{i=1}^N s_i / N$ .

Our main objective is to determine the zero-field magnetic susceptibility  $\chi$  that exhibits the power-law relation  $\chi(T) \propto |T - T_c|^{-\gamma}$  near the critical temperature  $T_c$ . The susceptibility for a finite system size can be expressed as a function of the order parameter  $m$  as

$$\chi(T, N) = \frac{N \langle m^2 \rangle}{k_B T}, \quad (7)$$

or alternatively,

$$\chi'(T, N) = N \frac{\langle m^2 \rangle - \langle |m| \rangle^2}{k_B T}. \quad (8)$$

Despite the difference in their definitions, both  $\chi$  and  $\chi'$  yield the same critical exponent  $\gamma$  by the finite-size scaling method, as described in Ref [36]. The expectation values  $\langle |m| \rangle$  and  $\langle m^2 \rangle$  at temperature  $T$  are evaluated by canonical MC simulations [36, 37]. Sampling of the configurational space was carried out by using the single-cluster update algorithm [38] which prevents the critical slowing down near the transition.

Quantitative evaluation of critical exponents can be achieved by using the finite-size scaling technique [39, 40, 41]. Close to the critical temperature  $T_c$ , the susceptibility for a finite system size satisfies the following scaling behaviour:

$$\chi(T, N) \propto N^{\gamma/\mu} \cdot \chi_0(|T - T_c|N^{1/\mu}). \quad (9)$$

Here,  $\mu$  is the critical exponent describing the divergence of the correlation volume  $\xi_V(T)$  of the order parameter:

$$\xi_V(T) \propto |T - T_c|^{-\mu}. \quad (10)$$

The quantity  $\xi_V$  is a natural generalization [23, 42] of the correlation length  $\xi$  that diverges as  $\xi(T) \propto |T - T_c|^{-\nu}$  with the critical exponent  $\nu$  in the planar model. Near  $T_c$ , the argument of the scaling functions  $\chi_0$  in (9), denoted by  $x = |T - T_c|N^{1/\mu}$ , becomes much smaller than unity. This allows the polynomial expansion of the scaling function  $\chi_0$  as

$$\chi(T, N) = a_0 N^{\gamma/\mu} + a_1 |T - T_c| N^{(1+\gamma)/\mu} + \dots + a_n |T - T_c| N^{(n+\gamma)/\mu}, \quad (11)$$

terminating the expansion at the order  $n$ . By substituting the numerical data of  $\chi(T, N)$  and their corresponding values of  $T$  and  $N$  into (11), followed by performing the nonlinear least square fitting, we obtain the critical exponents  $\gamma$  and  $\mu$  and the critical temperature  $T_c$  as optimal fitting parameters.

## 5. Results

### 5.1. Susceptibilities and critical exponents for $\Delta r = 0$

Before addressing the bulk critical properties, we first demonstrate the results for entire heptagonal lattices with  $\Delta r = 0$  (boundary contributions are fully involved). Figure 3(a) and 3(b) show the calculated results of the zero-field susceptibilities  $\chi(T, N)$  and  $\chi'(T, N)$ , respectively, as a function of temperature  $T$ . The single logarithmic plot is used in the figure 3(a). The system size  $r = r_{\text{in}}$  is varied from 4 to 8, which corresponds to the change in the number of total sites from  $N = 315$  to  $N = 15435$ . Both  $\chi$  and  $\chi'$  exhibit such a typical behaviour that indicates the occurrence of a ferromagnetic transition within the temperature range of  $1.1 \leq T \leq 1.3$ . For instance, the  $\chi$  curve in figure 3(a) monotonically increases with a decrease in  $T$ ; this is attributed to the onset



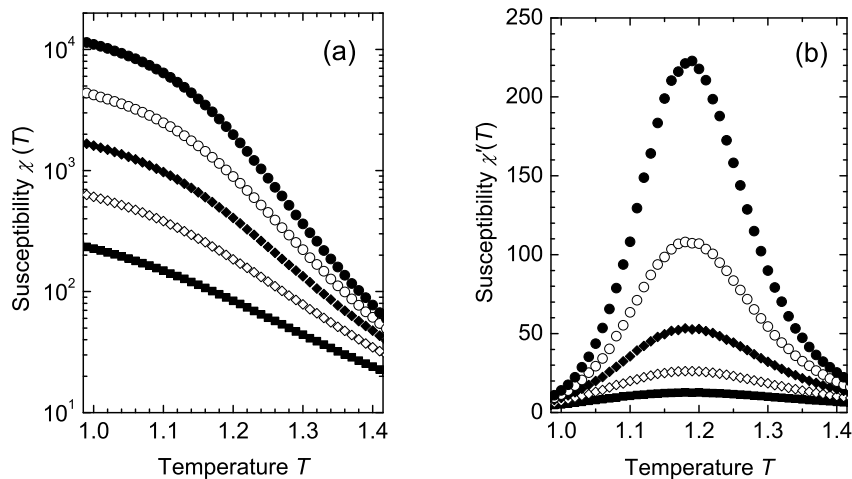


**Figure 3.** (a) Zero-field magnetic susceptibilities: (a)  $\chi(T, N)$  and (b)  $\chi'(T, N)$ , for entire heptagonal lattices with  $\Delta r = 0$ . The system size is varied from  $r_{\text{in}} = 4$  (square) to  $r_{\text{in}} = 8$  (solid circle), which corresponds to the change in the number of total sites from  $N = 315$  to  $N = 15435$ .

of the ordered phase. As well, the plot of  $\chi'$  in figure 3(b) exhibits a sharp peak at  $T \sim 1.2$ , which is also a precursor of the divergence in the infinite system.

Figure 4 (a) shows the scaling plot of  $\chi(T, N)$  based on (9). The vertical and horizontal axes represent the scaled susceptibility  $\chi(x)N^{-\gamma/\mu}$  and its argument  $x \equiv |T - T_c|N^{1/\mu}$ , respectively. The critical exponents evaluated from the upper and lower branches are  $\gamma = 2.28(2)$  and  $\mu = 3.46(1)$ , and  $\gamma = 2.26(2)$  and  $\mu = 3.47(1)$ , respectively. The errors in the last decimal places, which are shown in parentheses, designate a 95% confidence interval. As expected, the estimated values of  $\gamma$  and  $\mu$  for the two branches are in agreement within numerical errors. The optimal value of the critical temperature for the two branches is evaluated as  $T_c = 1.253(1)$ ; this agrees with the preceding estimation from the values of figures 3(a) and 3(b). A similar analysis for  $\chi'$  results in  $\gamma = 2.26(3)$ ,  $\mu = 3.45(2)$ , and  $T_c = 1.254(2)$ ; these values are fully consistent with the results deduced from the data of  $\chi$ .

We re-emphasize the fact that for regular Ising lattices embedded on curved surfaces,  $N$  instead of  $r$  should be adopted as the scaling variable. This is justified by attempting the finite size scaling of  $\chi$  using  $r$ . Figure 4(b) presents the scaling plot of  $\chi$  in terms of another scaling argument  $y = |T - T_c|r^{1/\mu'}$ ; the estimated values of the parameters are  $\gamma' = 1.8(3)$ ,  $\mu' = 2.0(4)$ , and  $T_c = 1.46(4)$ . It is evident that the data points do not collapse onto a single curve, but instead exhibit a large scatter. Furthermore, the resulting value of  $T_c$  differs from the temperature at which the susceptibility  $\chi'(T)$  exhibits a sharp peak (see figure 3). These facts indicate that the linear dimension  $r$  is not a characteristic length scale that describes the scaling behaviour of the thermodynamic quantities for curved surfaces.

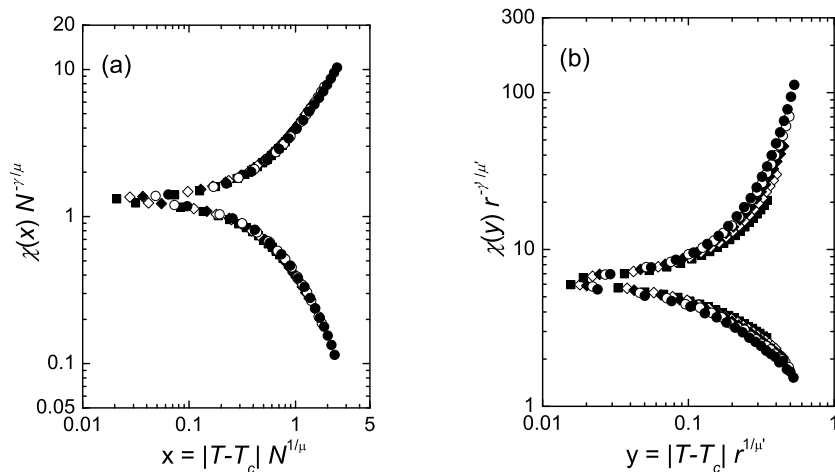


**Figure 4.** (a) Scaling plot of  $\chi(T, N)$  against the argument  $x = |T - T_c| N^{1/\mu}$ . The optimal values of critical exponents are  $\gamma = 2.28(2)$  and  $\mu = 3.46(1)$ , and  $\gamma = 2.26(2)$  and  $\mu = 3.47(1)$  for the upper and lower branches, respectively. The critical temperature is estimated as  $T_c = 1.253(1)$  for the two branches. (b) Scaling attempts of  $\chi$  against the alternative argument  $y = |T - T_c| r^{1/\mu'}$  instead of  $x$ . Optimal values of parameters are  $\gamma' = 1.8(3)$ ,  $\mu' = 2.0(4)$ , and  $T_c = 1.46(4)$ .

### 5.2. Critical exponents for $\Delta r > 0$ : Boundary effects

We now turn to the study of bulk critical properties of the heptagonal Ising lattice model. As mentioned in Sec. 3, the boundary spins of Ising lattices on a pseudosphere are thought to affect significantly to the nature of the system, since the number of the spins along the boundary increases as fast as that of total spins of the lattice. Hence, in order to extract the bulk critical exponents, we must try to remove the contribution of the boundary spins to the scaling behavior of the system. This is achieved by setting the disregarded layers  $\Delta r = r_{\text{out}} - r_{\text{in}}$  to be finite, i.e., by summing up only the spins within the interior  $r_{\text{in}}$  layers when performing MC simulations on the systems consisting of  $r_{\text{out}} (> r_{\text{in}})$  layers. If  $\Delta r$  is sufficiently large, the ensemble of the spins involved in the interior  $r_{\text{in}}$  layers may yield the critical exponents of the bulk system that is free from the boundary contribution.

On the basis of the argument above, we have prepared the heptagonal lattices having various values of  $r_{\text{in}}$  and  $\Delta r$ , and systematically employed the scaling analysis to them. It then reveals how the critical exponents  $\gamma$  and  $\mu$  and the critical temperature  $T_c$  depend on the number of disregarded layers  $\Delta r$ . The calculated results are given in Figure 5 (a) and 5 (b); each data point in the plots was extracted by means of the finite size scaling analysis for the system sizes  $4 \leq r_{\text{in}} \leq 8$ . (Hence, the maximum system size we have treated reaches  $r_{\text{out}} = 12$  which corresponds to  $N = 725760$ .) We found that an increase in  $\Delta r$  results in a monotonic decrease in all quantities in question:  $\gamma$ ,  $\mu$  and  $T_c$ , which indicates the significant contribution of the boundary spins to the scaling

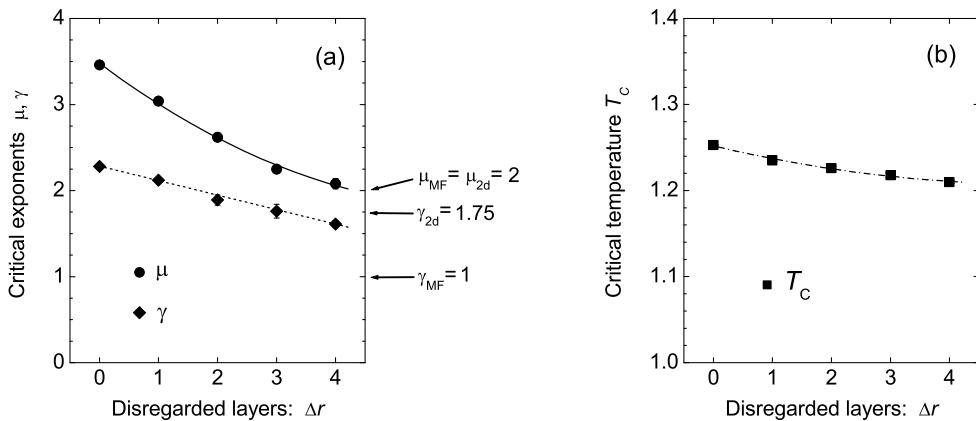


**Figure 5.** (a)  $\Delta r$ -dependences of the critical exponents  $\gamma$  and  $\mu$ , and (b) that of the critical temperature  $T_c$ . The lines in the plots serve as a guide to eye. Each data point was extracted by means of the finite size scaling analysis for the system sizes  $4 \leq r_{in} \leq 8$ . The values of the mean-field exponents  $\gamma_{MF}$  and  $\mu_{MF}$  are indicated in the plot (a).

behavior of the system.

Asymptotic behavior of the curves of  $\gamma$  and  $\mu$  for large  $\Delta r$  provide estimations of the bulk critical exponents. From Figure 5 (a), we see that the curve of  $\mu$  shows somewhat convergence to a particular value of  $\mu \sim 2$  or less. Since this is close to the value of  $\mu$  for the two-dimensional planar Ising model<sup>||</sup>,  $\mu_{2d} = 2$ , it appears that the bulk system attains the planar Ising universality class at around  $\Delta r \sim 4$ . However, the asymptotic behavior of  $\gamma$  is slightly different from that of  $\mu$ ; while the value of  $\gamma$  equals to that of the planar system  $\gamma_{2d} = 1.75$  at  $\Delta r \sim 3$ , it still continues to decrease almost linearly with  $\Delta r$  and thus has no tendency to converge to  $\gamma_{2d}$  for large  $\Delta r$ . Thereby, the bulk critical exponent  $\gamma$  will be smaller than  $\gamma_{2d}$ , which suggests that the heptagonal Ising lattice belongs to some other universality class than of the planar Ising lattices.

In the context above, the asymptotic value  $\mu \sim 2$  for large  $\Delta r$  is not the exponent  $\mu_{2d}$  but another specific exponent characterizing the intrinsic nature of the system. This point is clarified by referring to the previous studies done by Rietman *et al.* [21] and by Doyon and Fonseca [22]. They both have stated that the Ising lattice model embedded on the pseudosphere should yield the mean-field critical exponents when the boundary contribution may be omitted. The mean-field nature of the system is attributed to the fact that an Ising lattice embedded on a pseudosphere is effectively an infinite dimensional lattice at large distance due to the exponential growth of the total spins [43]. For an ordinary Ising lattice in  $d$  dimension, the number of spins along the boundary,  $N_s$ , is related to that of the total spins  $N$  as  $N_s \propto N^{1-(1/d)}$ . Hence,

<sup>||</sup> The value  $\mu_{2d} = 2$  is derived from the relation  $\mu = \nu d$  (See (11)) and the exact solution  $\nu = 1$  for  $d = 2$ .

the peculiar relation  $N_s \propto N$  that holds on negatively curved surfaces consequences  $d = \infty$ . Accordingly, our heptagonal Ising lattices are expected to yield the mean-field critical exponents  $\gamma_{\text{MF}} = 1$  and  $\mu_{\text{MF}} = 2$ , where  $\mu_{\text{MF}}$  is determined by  $\mu_{\text{MF}} = \nu_{\text{MF}} d_c$  as suggested in Ref. [23]. Our numerical results given in Figure 5 (a) is in fact qualitatively consistent with the argument above; that is,  $\mu$  converges to  $\mu_{\text{MF}} = 2$  for  $\Delta r \geq 4$ , and  $\gamma$  continues to decrease until it yields  $\gamma_{\text{MF}} = 1$ . (To be precise, the asymptotic value of  $\gamma$  may take the value between  $\gamma_{2d}$  and  $\gamma_{\text{MF}}$  depending on the numerical conditions; this point will be discussed in Section 6 in detail.)

### 5.3. Binder's cumulant $U_4(T, N)$

We have also carried out an alternative estimation of  $T_c$  and  $\mu$  in terms of the fourth-order Binder's cumulant  $U_4(T, N)$  defined by [36, 37, 44]

$$U_4(T, N) = 1 - \frac{\langle m^4 \rangle}{3\langle m^2 \rangle^2}. \quad (12)$$

For a given  $N$ , the cumulant  $U_4(T)$  decreases monotonically with an increase in  $T$  from  $U_4(0) = 2/3$  to  $U_4(\infty) = 0$ . In the vicinity of  $T_c$ , the  $T$ -dependence of it can be approximated by

$$U_4(T, N) = U^{(0)} + U^{(1)} \left(1 - \frac{T}{T_c}\right) N^{1/\mu}, \quad (13)$$

where  $U^{(0)}$  and  $U^{(1)}$  are constants and are thus independent of  $T$  and  $N$ . The expression (13) is a direct consequence of the assumption that the probability distribution of the order parameter  $m$  should be Gaussian close to the transition [36]. From (13), it follows

$$U_4(T_c, N) = \text{const.} \quad \text{and} \quad \left. \frac{dU_4}{dT} \right|_{T=T_c} \propto -N^{1/\mu}, \quad (14)$$

which provides a complementary method to estimate  $T_c$  and  $\mu$ .

Figures 6 (a)-(c) present the numerical results for  $U_4(T, N)$  for several values of  $\Delta r$ . In each plot, we found a unique crossing point giving an estimate of the critical temperature as  $T_c \simeq 1.25, 1.22$  and  $1.20$  for  $\Delta r = 0, 2$  and  $4$ , respectively. These values of  $T_c$  are in fair agreement with those obtained by the scaling analyses for the susceptibilities presented in Figure 5 (b).

Figure 6 (d) shows the  $N$  dependence of the derivative with negative sign  $-dU_4/dT$  at  $T = T_c$  for different  $\Delta r$ . The magnitude of the derivative grows with a power-law with increasing  $N$  as expected from (14). The estimates of  $\mu$  are  $\mu \sim 3.6, 7.7, 12.5$  for  $\Delta r = 0, 2, 4$ , respectively. It should be noted that these values of  $\mu$  increase with  $\Delta r$ . This clearly contradicts to the results of the scaling analyses on the susceptibility  $\chi$  (See Fig. 5 (a)), where  $\mu$  is found to be such a decreasing function of  $\Delta r$  that yields the mean-field value  $\mu_{\text{MF}} = 2$  in the large  $\Delta r$  limit. The discrepancy may be due to simply a finite sized effect; or, it may indicate some intrinsic property of negatively curved

¶ For the Ising model, the mean-field exponent  $\nu_{\text{MF}}$  is  $1/2$ , and the upper critical dimension  $d_c$  is  $4$ ; thus we obtain  $\mu_{\text{MF}} = 2$ .

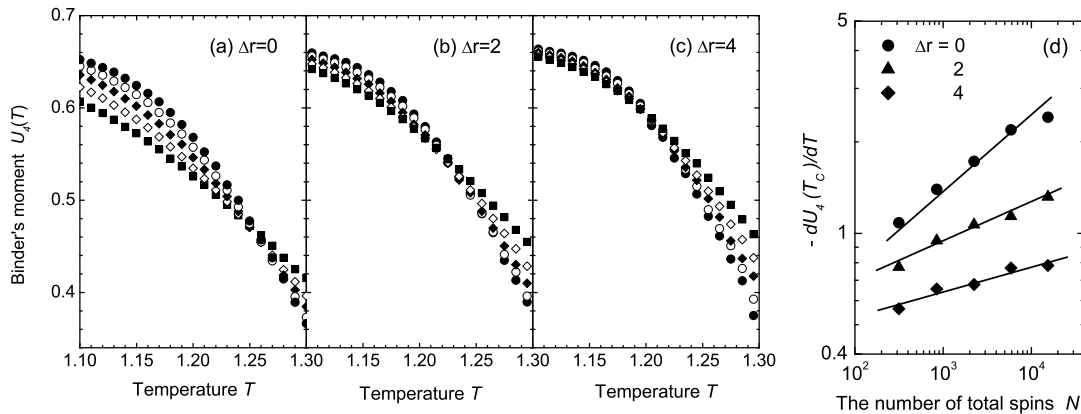


**Figure 6.** (a)-(c) Temperature dependences of the fourth-order Binder's cumulant  $U_4(T, N)$  for various values of  $\Delta r$ . The size of the interior layers is varied from  $r_{\text{in}} = 4$  (square) to  $r_{\text{in}} = 8$  (solid circle). (d) The negative slope of the cumulant,  $-dU_4/dT|_{T=T_c}$ , for each value of  $\Delta r$ . The solid lines represent the power-law ( $\propto N^{1/\mu}$ ) with  $\mu = 3.6, 7.7$ , and  $12.5$  from top to bottom.

surfaces with regard to the distribution of the order parameter  $m$ , since the power-law relation (14) originate from the assumption of the Gaussian distribution of  $m$  [36]. More through discussion about this point will be presented elsewhere.

## 6. Discussions and Concluding remarks

Our numerical analysis revealed that the critical exponents  $\gamma$  and  $\mu$  of the heptagonal Ising model defined on negatively curved surfaces assume values that deviate from those for the planar Ising model. Most striking is that, when reducing the contribution of spins near the boundary, both  $\gamma$  and  $\mu$  exhibit a tendency to yield the mean-field exponents. This phenomenon is attributed to the fact that the regular Ising lattices on negatively curved surfaces serve as an effectively infinite dimensional lattices due to the peculiarity of the intrinsic geometry.

The above statement immediately poses the following question: Does the negative curvature of the underlying geometry alter the other four critical exponents? With regard to the power-law behaviour of thermodynamic quantities, the planar Ising model is known to possess four other critical exponents [4]:  $\alpha = 0$ ,  $\beta = 1/8$ ,  $\delta = 15$ , and  $\eta = 1/4$ , which correspond to heat capacity, spontaneous magnetization, critical isotherm, and the two-point correlation function, respectively. Our preliminary study [45] has suggested that, the exponent  $\beta$  for large  $\Delta r$  also tend toward the mean-field exponent  $\beta_{\text{MF}} = 1/2$ , whereas  $T_c$  estimated there is slightly different from that in the present work. Detailed analyses on this issue and the quantitative determination of the

other exponent  $\delta$  (and  $\eta$ , if it exists<sup>+</sup>) will be given in a future study. Very recently, we have found that the dynamic critical exponent  $z$  in our heptagonal Ising model also shift quantitatively from that for the planar Ising model [46].

It deserves comment that the finite curvature of the underlying geometry may produce another type of effect wherein the spin variables at each site possess orientational degrees of freedom. This is because the relative angle of interacting spins at neighbouring sites on a curved surface is determined by a spatially-dependent metric tensor. Thus, the Hamiltonian of the system should be modified such that it is a function of the metric tensor. As a result, the energetically preferable configurations of the vector spins differ from those in planar systems [47, 48, 49, 50, 51], which implies that the critical behaviour of these vector-spin lattice models is markedly influenced by a finite surface curvature.

Further noteworthy is, however, the fact that the geometric curvature continues to be relevant to the critical behavior of the system despite the omission of the vector property of the interacting spin variables; this was demonstrated by our results. Evidently, the spin variable of our model is set to be a scalar, and thus the Ising Hamiltonian given by (6) is devoid of the metric factor. Nevertheless, the surface curvature is surely relevant to the Ising model on curved surfaces since it enables to construct peculiar lattice structures that cannot be realize in a flat plane. This means that the surface curvature induces the alteration of the global symmetry of the system even when the interacting entities do not exhibit any vector property. Besides, in the vicinity of the critical point, the discreteness of the lattice becomes irrelevant and the model can be considered to be a continuum surface with a constant curvature. Therefore, the metric of the underlying geometry plays a crucial role in the scaling behaviour of the Ising lattice model defined on the surface. In this context, the mean-field nature of the critical exponents  $\gamma$  and  $\mu$  are expected to be universal for all lattice structures other than the heptagonal one; this point is being investigated.

We remark that it is also interesting to study the dependence of the values of the bulk critical exponents on the interior lattice size  $r_{\text{in}}$  we have introduced. Obviously, the condition  $1 \ll r_{\text{in}} \ll r_{\text{out}}$  is desirable to determine the bulk properties of the lattice with accuracy. If the  $r_{\text{in}}$  is not so large (compared to the curvature radius of the underlying surface), the system can be regarded as an Ising lattice defined on a nearly flat surface. Thereby, the resultant critical exponents will become comparable with those for the planar Ising lattice rather than the true bulk critical exponents (i.e., the mean-field exponents). This implies that, by gradually increasing the size of  $r_{\text{in}}$ , the system go through a crossover from the planar Ising class to the mean-field class. We conjecture that this crossover phenomenon is observed in the shift of the asymptotic value of  $\gamma$  deduced from the plot in Figure 5 (a); that is, when increasing the size of  $r$  employed in the analyses, the asymptotic value of  $\gamma$  at  $\Delta r \gg 1$  will shift downward

<sup>+</sup> Rietman *et al.* [21] have suggested that the two-point correlation function of the Ising lattices on a pseudosphere shows an exponential decay instead of an power-law decay. If it is true, the critical exponent  $\eta$  can be no longer defined.

from  $\gamma \sim \gamma_{2d} = 1.75$  to  $\gamma \sim \gamma_{MF} = 1$ . Accordingly, it is possible that the curve of  $\gamma$  plotted in Figure 5 (a) converges to an intermediate value between  $\gamma_{2d}$  and  $\gamma_{MF}$  under the present numerical conditions.

In conclusion, we have investigated the critical behaviour of the Ising model defined on a curved surface with constant negative curvature. MC simulations and finite-size scaling analyses were employed to compute the critical exponent  $\gamma$  and  $\mu$  for the zero-field magnetic susceptibility and correlation volume, respectively. The resulting values  $\gamma$  and  $\mu$  show distinct values from those for the planar Ising model, and exhibit a tendency to the mean-field exponents  $\gamma_{MF} = 1$  and  $\mu_{MF} = 2$  due to the peculiar intrinsic geometry of the negatively curved surface. As well, we have revealed quantitatively how the boundary spins contribute to the determination of  $\gamma$ ,  $\mu$  and  $T_c$ , and argued the possibility to occur the crossover from the planar Ising class to the mean-field Ising class. We hope that the generalization our statistical model (with regard to the lattice structure, dimensionality of the embedding space, distribution of interacting strength, *etc.*) would unveil a wide variety of interacting critical properties of the physical systems assigned on general curved spaces.

## Acknowledgments

We thank T. Nakayama and K. Yakubo for useful discussions. This work was supported in part by a Grant-in-Aid for Scientific Research from the Japan Ministry of Education, Science, Sports and Culture. One of the authors (HS) is thankful for the financial support from the 21st Century COE “Topological Sciences and Technologies,” and for the conversation with S. Tanda, Y. Asano, and K. Konno. Numerical calculations were performed in part on the Supercomputer Center, ISSP, University of Tokyo.

## Appendix A. The pseudosphere

The pseudosphere is defined as one sheet of the double-sheeted hyperboloid [19]

$$x^2 + y^2 - z^2 = -1, \quad (\text{A.1})$$

possessing the Minkowskian metric  $ds^2 = dx^2 + dy^2 - dz^2$ . Since (A.1) specifies the locus of points whose squared distance from the origin are equal to  $-1$ , it is called a *pseudosphere* having the radius  $i = \sqrt{-1}$  by analogy with the sphere.

While the above definition is rigorous, it is clumsy for computations since three coordinates are used for only two degrees of freedom. This cumbrousness is removed by using an alternative representation of the pseudosphere, called the Poincaré disk model [29]. Suppose that the upper hyperboloid sheet is projected onto the  $x$ - $y$  plane using the following mapping:

$$(x, y, z) \rightarrow \left( \frac{x}{1+z}, \frac{y}{1+z} \right). \quad (\text{A.2})$$

This transforms the upper sheet to a unit circle endowed with the metric

$$ds^2 = w^2(dx^2 + dy^2), \quad w = \frac{2}{1-x^2-y^2}. \quad (\text{A.3})$$

The unit circle possessing the metric (A.3) is referred to as a Poincaré disk, and it serves as a compact representation of the pseudosphere. The boundary of the disk corresponds to the points at infinity of the hyperboloid. The Gaussian curvature  $\kappa$  on the disk is calculated using the formula:

$$\kappa = -\frac{1}{w^2} \left( \frac{\partial^2}{\partial x^2} + \frac{\partial^2}{\partial y^2} \right) \ln w. \quad (\text{A.4})$$

From (A.3) and (A.4), we see that  $\kappa = -1$  at arbitrary points on the disk. Thus it follows that the pseudosphere is a curved surface with a constant negative curvature  $\kappa = -1$ .

## References

- [1] Kadanoff L P 1966 *Physics* **2** 263
- [2] Wilson K G 1971 *Phys. Rev. B* **4** 3174
- [3] Cardy J, 1996 *Scaling and Renormalization in Statistical Physics* (Cambridge University Press, Cambridge UK)
- [4] Fisher M E 1998 *Rev. Mod. Phys.* **70** 653
- [5] Nakayama T and Yakubo K 2003 *Fractal Concepts in Condensed Matter Physics* (Springer).
- [6] Onsager L 1944 *Phys. Rev.* **65** 117
- [7] Kaufman B 1949 *Phys. Rev.* **76** 1232
- [8] McCoy B M and Wu T T *The Two-Dimensional Ising Model* (Harvard University Press, Cambridge MA) 1973
- [9] Izmailian N Sh and Hu C -K 2002 *Phys. Rev. E* **65** 036103
- [10] Diego O, Gonzalez J and Salas J 1994 *J. Phys. A: Math. Gen.* **27** 2965
- [11] Hoelbling Ch and Lang C B 1996 *Phys. Rev. B* **54** 3434
- [12] González J 2000 *Phys. Rev. E* **61** 3384
- [13] Weigel M and Janke W 2000 *Europhys. Lett.* **51** 578



- [14] Deng Y and Blöte H W J 2003 *Phys. Rev. E* **67** 036107
- [15] Costa-Santos R 2003 *Phys. Rev. B* **68** 224423
- [16] Ferdinand A E and Fisher M E 1969 *Phys. Rev.* **185** 832
- [17] Janke W and Kenna R 2002 *Phys. Rev. B* **65** 064110
- [18] Izmailian N Sh, Oganessian K B and Hu C -K 2002 *Phys. Rev. E* **65** 056132
- [19] Coxeter H S M, 1969 *Introduction to Geometry* (Wiley, New York).
- [20] Firby P A and Gardiner C F 1991 *Surface Topology* (Ellis Horwood, London)
- [21] Rietman R, Nienhuis B and Oitmaa J 1992 *J. Phys. A: Math. Gen.* **25** 6577
- [22] Doyon B and Fonseca P 2004 *J. Stat. Mech.* P07002
- [23] Botet R, Jullien R and Pfeuty P 1982 *Phys. Rev. Lett.* **49** 478
- [24] Avron J E, Klein M, Pnueli A and Sadun L 1992 *Phys. Rev. Lett.* **69** 128
- [25] Iengo R and Li D 1994 *Nucl. Phys. B* **413** 735
- [26] Pnueli A 1994 *Ann. Phys.* **231** 56
- [27] Alimohammadi M and Sadjadi H M 1999 *J. Phys. A: Math. Gen.* **32** 4433
- [28] Bulaev D V, Geyler V A and Margulis V A 2003 *Physica B* **337** 180
- [29] Balazs N L and Voros A 1986 *Phys. Rep.* **143** 109
- [30] Grosche C 1992 *J. Phys. A: Math. Gen.* **25** 4573
- [31] Stöckmann H -J 1999 *Quantum Chaos: An Introduction* (Cambridge University Press, Cambridge UK)
- [32] D'Hoker E and Phong D H 1988 *Rev. Mod. Phys.* **60** 917
- [33] Levin J 2002 *Phys. Rep.* **365** 251
- [34] Elser V and Zeng C 1993 *Phys. Rev. B* **48** 13647
- [35] d'Auriac J C A, Mélin R, Chandra P and Douçot B 2001 *J. Phys. A: Math. Gen.* **34** 675
- [36] Binder K and Heermann D W 2002 *Monte Carlo simulation in Statistical Physics*, (Springer)
- [37] Landau D P and Binder K 2000 *A Guide to Monte Carlo Simulations in Statistical Physics* (Cambridge University Press)
- [38] Wolff U 1989 *Phys. Rev. Lett.* **62** 361
- [39] Fisher M E and Barber M N 1972 *Phys. Rev. Lett.* **28** 1516
- [40] Cardy J L 1988 *Finite-Size Scaling* (Elsevier Science)
- [41] Privman V 1990 *Finite Size Scaling and Numerical Simulation of Statistical Systems* (World Scientific Pub)
- [42] Pękałski A 2001 *Phys. Rev. E* **64** 057104
- [43] Callan C and Wilczek F 1990 *Nucl. Phys. B* **340** 366
- [44] Binder K 1981 *Z. Phys. B* **43** 119; Binder K 1981 *Phys. Rev. Lett.* **47** 693
- [45] Sakaniwa Y and Shima H, *to be published*.
- [46] Shima H and Sakaniwa Y, cond-mat/0512167.
- [47] Saxena A and Dandoloff R 1997 *Phys. Rev. B* **55** 11049
- [48] Balakrishnan R and Saxena A 1998 *Phys. Rev. B* **58** 14383
- [49] Freitas W A, Moura-Melo W A and Pereira A R 2005 *Phys. Lett. A* **336** 412
- [50] Pereira A R 2005 *J. Magn. Magn. Mater.* **285** 60
- [51] Moura-Melo W A, Pereira A R, Mól L A S and Pires A S T [cond-mat/0511443]